

## Phase relations in superconductor–normal metal–superconductor tunnel junctions

Yu. S. Barash

*Institute of Solid State Physics of the Russian Academy of Sciences, 2 Academician Ossipyan Street, Chernogolovka, Moscow District 142432, Russia* (Received 2 January 2019; revised manuscript received 1 March 2019; published 22 April 2019)

The phase difference  $\phi$ , between the superconducting terminals in superconductor–normal metal–superconductor tunnel junctions (SINIS), incorporates the phase differences  $\chi_{1,2}$  across thin interfaces of constituent SIN junctions and the phase incursion  $\varphi$  between the side faces of the central electrode of length  $L$ . It is demonstrated here that  $\chi_{1,2}$  pass through over their proximity-reduced domain twice, there and back, while  $\phi$  changes over the single period. Two corresponding solutions, that describe the double-valued order-parameter dependence on  $\chi_{1,2}$ , jointly form the single-valued dependence on  $\phi$ , operating in two adjoining regions of  $\phi$ . The phase incursion  $\varphi$  plays a crucial role in creating such a behavior. The current-phase relation  $j(\phi, L)$  is composed of the two solutions and, at a fixed small  $L$ , is characterized by the phase-dependent effective transmission coefficient.

DOI: [10.1103/PhysRevB.99.140508](https://doi.org/10.1103/PhysRevB.99.140508)

**Introduction.** When two superconductors are separated by a thin interface, their phase-dependent Josephson coupling generates the Josephson supercurrent through the junction [1–3]. If a normal metal is placed between the superconductors with nonzero interface transparencies [superconductor-interface-normal metal-interface-superconductor (SINIS)], their Josephson coupling appears as a corollary of the proximity-induced superconducting correlations in the normal-metal region [4–8]. Various hybrid systems, in which the Josephson coupling through normal-metal electrodes is induced by the proximity effect, have recently been the focus of research activities [9–20].

A SINIS junction (see Fig. 1) is characterized by the phase difference  $\phi$  between the superconducting terminals, which can be represented as the sum of internal phase differences  $\chi_{1,2}$ , across the interfaces of two constituent SIN junctions, and the supercurrent-induced phase incursion  $\varphi$  between side faces of the central electrode of length  $L$ :  $\phi = \chi_1 + \chi_2 + \varphi$ . This Rapid Communication develops a theory of symmetric SINIS tunnel junctions within the Ginzburg-Landau (GL) approach that allows one to describe the proximity effects of the Josephson origin on the phases mentioned above, and consequently on the junction's characteristics.

For the junctions in question, one usually gets  $\chi_{1,2} = \chi$  in equilibrium. The internal phase difference  $\chi$  could be controlled by the magnetic flux through an auxiliary superconducting ring involving only the constituent SIN contact, where the normal-metal lead is in the proximity-induced superconducting state. However, it is  $\phi$  that is commonly used as a control parameter in experiments and establishes both  $\chi(\phi, L)$  and  $\varphi(\phi, L)$ . It will be demonstrated below that  $\chi$ , as opposed to  $\phi$ , does not determine the junction state uniquely at a given  $L$ . For this reason  $\phi(\chi, L)$  and the order parameter absolute value represent the double-valued functions of  $\chi$ .

There are two solutions to the GL equation that come up since the equation cannot be linearized, even when the order parameter is very small in the given problem. Such a linearization is known to represent the simplest and most effective way of describing the problems of  $H_{c2}$  and  $H_{c3}$  [21–23] as well as some proximity effects in the vicinity of the superconductor–normal metal boundaries [24,25]. However, the linearization becomes impossible in the presence of a sizable gauge invariant gradient of the order parameter phase, i.e., the superfluid velocity. After switching over from  $\chi$  to  $\phi$ , the two found solutions operate in different regions  $|\phi| \leq \phi_*(L)$  and  $\phi_*(L) \leq |\phi| \leq \pi$ , within the period, adjoining at the points  $\phi = \pm\phi_*(L)$ . The phase incursion  $\varphi$  plays a crucial role in creating such a behavior. As a corollary, the current-phase relation  $j(\phi, L)$  is composed of the two solutions and its dependence on the transparency, at small  $L$ , gradually changes with  $\phi$  due to the phase incursion effects.

The influence of interfacial proximity effects in SINIS junctions on the phase relations, that results in a nonmonotonic dependence  $\chi(\phi, L)$  at a fixed  $L$ , has not been identified in the literature until now. The relation was typically simplified assuming negligible values of either the phase incursion  $\varphi$  over the central lead, or the phase drops  $\chi$  across thin interfaces. More advanced earlier attempts of describing the SNS junction within the GL approach [26,27] focused on the phase incursion and fully transparent interfaces, but were based on the specific boundary conditions and gave no

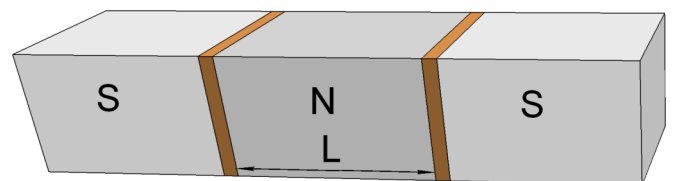


FIG. 1. Schematic diagram of the SINIS junction.

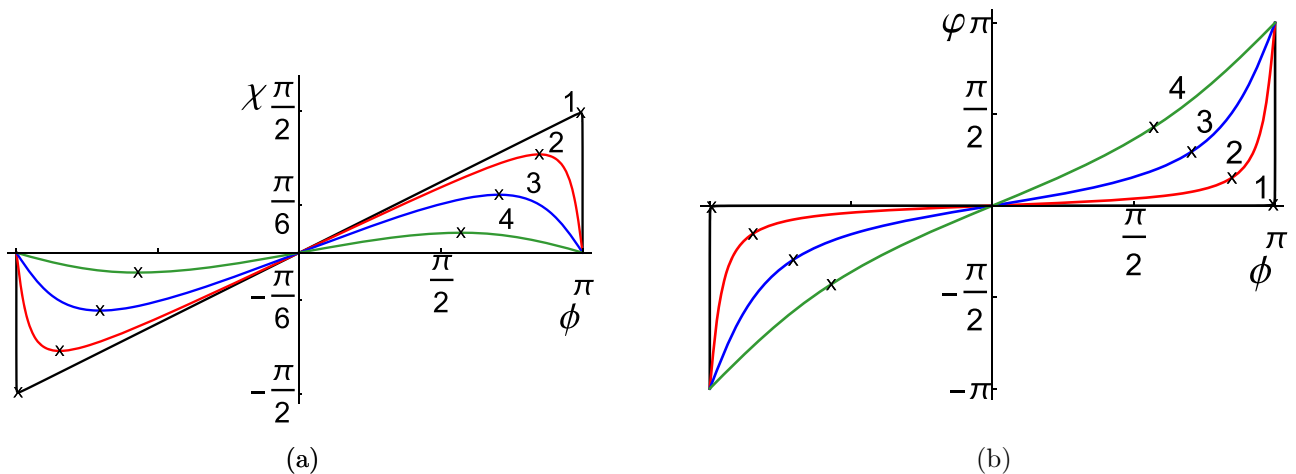


FIG. 2. The internal phase difference  $\chi$  (a) and the phase incursion  $\varphi$  (b) as functions of the phase difference  $\phi$  taken at various distances  $l$ : (1)  $l = 0.02$ , (2)  $l = 0.5$ , (3)  $l = 1.1$ , (4)  $l = 2.2$ .

consideration to the phase drops [28]. On the other hand, microscopic theories of the double-junction systems, being elaborated on and applied to a wide temperature range down to zero temperature [8,29–31], usually assume a negligible current-induced phase incursion in contrast to the phase drops. While the latter point is justified for SIS junctions in a wide range of realistic parameters, the range gets narrower in SINIS junctions, allowing both quantities  $\chi$  and  $\varphi$  to be of importance in the current transport at mesoscopic values of  $L$ , as shown below.

*Description of the model.* Consider a symmetric tunnel SINIS junction with two identical thin interfaces set at distance  $L$  on the side faces of the central normal metal lead (see Fig. 1). A one-dimensional spatial profile of the order parameter will establish itself in the system, if, for example, the electrodes' transverse dimensions are much less than both the superconductor coherence length  $\xi$  and the decay length  $\xi_n$  in the central electrode. The system's free energy involves the bulk and interface contributions  $\mathcal{F} = \sum \mathcal{F}_p + \mathcal{F}_n + \mathcal{F}_{\frac{L}{2}}^{\text{int}} + \mathcal{F}_{-\frac{L}{2}}^{\text{int}}$ . Here,  $p = 1, 2$  refer to the external superconducting electrodes, while subscript  $n$  refers to the central normal-metal lead. Assuming the latter to be described within the GL approach [32], one gets per unit area of the cross section

$$\mathcal{F}_n = \int_{-L/2}^{L/2} dX \left[ K_n \left| \frac{d}{dX} \Psi(X) \right|^2 + a_n |\Psi(X)|^2 + \frac{b_n}{2} |\Psi(X)|^4 \right], \quad (1)$$

where  $K_n, a_n, b_n > 0$  and the interfaces are placed at  $X = \pm L/2$ . The expressions for  $\mathcal{F}_{1,2}$  are obtained from (1) after substituting  $K_n, a_n, b_n \rightarrow K, -|a|, b$  and replacing the integration period  $(-L/2, L/2)$  by  $(-\infty, -L/2)$  or  $(L/2, \infty)$  for  $p = 1$  or  $2$ , respectively.

The interfacial free energy per unit area is

$$\mathcal{F}_{\pm \frac{L}{2}}^{\text{int}} = g_J |\Psi_{\pm \frac{L}{2}+} - \Psi_{\pm \frac{L}{2}-}|^2 + g |\Psi_{\pm \frac{L}{2}\pm}|^2 + g_n |\Psi_{\pm \frac{L}{2}\mp}|^2. \quad (2)$$

The first invariant in (2) describes the Josephson coupling while other terms take account of the interfacial pair breaking  $g > 0, g_n > 0$ .

The GL equation for the normalized absolute value of the order parameter in the central electrode  $\Psi = (a_n/b_n)^{1/2} f e^{i\alpha}$  takes the form

$$\frac{d^2 f}{dx^2} - \frac{i^2}{f^3} - f - f^3 = 0. \quad (3)$$

Here,  $x = X/\xi_n$ ,  $\xi_n = (K_n/a_n)^{1/2}$ , and the dimensionless current density is  $i = \frac{2}{3\sqrt{3}}(j/j_{\text{dp}})$ , where  $j_{\text{dp}} = (8|e|a_n^{3/2}K_n^{1/2})/(3\sqrt{3}\hbar b_n)$ .

The boundary conditions for the complex order parameter, which follow from (1) and (2), agree with the microscopic results [8] near  $T_c$ , at all transparency values [33–35]. Introducing  $l = L/\xi_n$ , one gets, in particular,

$$\left( \frac{df}{dx} \right)_{l/2-0} = -(g_{n,\delta} + g_\ell) f_- + g_\ell \cos \chi f_+, \quad (4)$$

$$i = -f^2 \frac{d\alpha}{dx} = g_\ell f_- f_+ \sin \chi. \quad (5)$$

Here,  $\chi = \alpha(\frac{l}{2} - 0) - \alpha(\frac{l}{2} + 0)$ ,  $f_- = f_{l/2-0}$ ,  $f_+ = f_{l/2+0}$ , and the dimensionless coupling constants  $g_\ell = g_J \xi_n / K_n$ ,  $g_{n,\delta} = g_n \xi_n / K_n$ .

*The phase relations.* The proximity effect of the Josephson origin, associated with the term containing  $\cos \chi$  in (4), takes place under the condition  $g_\ell \cos \chi > 0$ , when the Josephson coupling bilinear contribution to the free energy  $\propto -2g_\ell f_- f_+ \cos \chi$  decreases with an appearance of a small nonzero order parameter  $f_-$  on one side of a thin interface, in the presence of  $f_+$  on the other side. For 0 junctions considered below,  $g_\ell > 0$ . Therefore, for superconductivity to appear in the central lead, the internal phase difference  $\chi$  should change within the proximity-reduced range,  $|\chi| \leq \chi_{\text{max}}(l) < \frac{\pi}{2}$ , which is defined, in general, modulo  $2\pi$ . If  $\chi$  were outside the range, the inverse proximity effect would prevent superconductivity to show up in the central lead.

Figures 2(a) and 2(b) show, respectively, the internal phase difference  $\chi$  and the phase incursion  $\varphi$ , taken at various  $l$  as functions of the phase difference  $\phi$  between the superconductor terminals. All the numerical results have been obtained by carrying out an evaluation of the GL equations' solutions

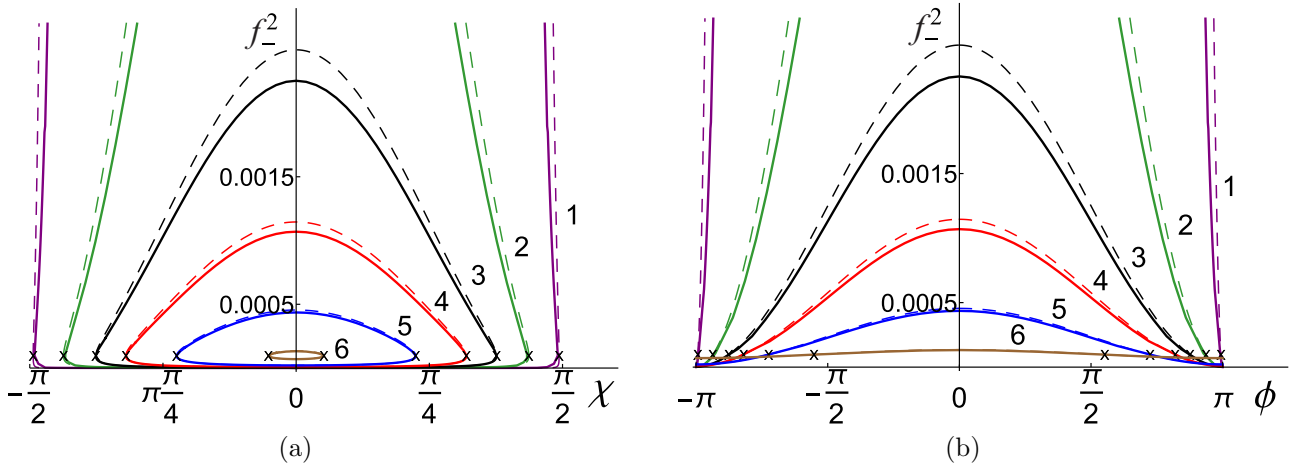


FIG. 3. The quantity  $f_-^2$  as (a) a double-valued function of  $\chi$  and (b) a single-valued function of  $\phi$  taken at various  $l$ : (1)  $l = 0.02$ , (2)  $l = 0.2$ , (3)  $l = 0.4$ , (4)  $l = 0.6$ , (5)  $l = 1$ , (6)  $l = 2.5$ .

that take into account the phase incursion and boundary conditions at interfaces with  $g_\ell = g_\delta = 0.01$  and  $g_{n,\delta} = 0$ , assuming  $K = K_n$ ,  $|a| = a_n$ , and  $b = b_n$ . The approximate analytical solutions for tunnel SINIS junctions have been also obtained [36]. They describe almost perfectly the functions  $\chi(\phi)$  and  $\varphi(\phi)$  for the parameter set chosen, with deviations from the numerical results that are indiscernible in Figs. 2(a) and 2(b).

If the phase incursion  $\varphi$  is negligibly small, one gets from  $\phi = 2\chi + \varphi$  a simple dependence  $\chi(\phi) = \frac{\phi}{2}$ , which results in the variation range  $|\chi| \leq \frac{\pi}{2}$  for  $|\phi| \leq \pi$ . Such a behavior takes place at sufficiently small distances  $l \ll 1$ , except for a narrow vicinity of  $\phi = \pi$ , as shown in curves 1 in Figs. 2(a) and 2(b). Curves 2–4 demonstrate that, in a wide range of  $\phi$ ,  $\chi$  is of importance at mesoscopic lengths  $l \lesssim 1$ , while a substantial influence of  $\varphi$  on the phase relations appears at  $l \gtrsim 1$ .

Since the supercurrent is spatially constant due to the presumed quasi-one-dimensional character of the problem, a local decrease of the Cooper pair density is accompanied by the increase of the superfluid velocity, i.e., of the gradient of the order parameter phase. Therefore, small local values of  $f$  result in a noticeable  $\varphi$ . Due to a spatial decay of the proximity-induced condensate density with increasing distances from the interfaces,  $\varphi$  increases with  $l$  at a given  $\phi$ , while the range of variation of  $|\chi| \leq \chi_{\max}(l)$  becomes smaller:  $\chi_{\max}(l) \approx \arccos(\tanh l)$ . At  $l \gg 1$ ,  $f$  is especially small in the depth of the central electrode,  $\varphi$  dominates the right-hand side in  $\phi = 2\chi + \varphi$ , while  $|\chi|$  is greatly reduced.

Figure 2(a) demonstrates that  $\chi$  is a nonmonotonic function of  $\phi$  that passes through over the proximity-reduced region twice, there and back, while the phase difference  $\phi$  between the superconducting terminals changes over the period. Two different values of  $\phi$  at one and the same  $\chi$  are linked to the different phase incursions and, more generally, to the two solutions of the GL equation for the absolute value of the order parameter, taken at a given  $\chi$ . The dots marked with crosses represent in all the figures the points of contact

of the two solutions, i.e., indicate the corresponding quantities taken at  $\chi = \pm\chi_{\max}(l)$ .

*The order parameter  $f_-$ .* The nonlinear term  $i^2 f^{-3} \propto v_s^2(x) f(x)$  [where the superfluid velocity is  $v_s(x) \propto i/f^2$ ] cannot, as a rule, be disregarded in (3) as compared to the linear one. In the depth of the central lead it dominates the latter, when  $\phi$  is close to  $\pi$ . For this reason the GL equation (3) remains nonlinear even if the cubic term is negligible in the problem under consideration. As a result, there are two basic solutions for  $f$  at a given  $\chi$ .

The normalized order-parameter absolute value squared  $f_-^2$  taken at a side face of the central electrode is shown in Figs. 3(a) and 3(b) at various  $l$  as a function of  $\chi$  and  $\phi$ , respectively. The analytical description (dashed curves), that assumes the conditions  $f_- \sim g_\ell f_+ \ll 1$  and  $g_{n,\delta} \lesssim g_\ell$ , approximates the numerical results shown reasonably well. As distinct from the phase relations in Fig. 2, the solid and dashed curves in Fig. 3 can be, mostly, clearly distinguished. The two solutions adjoin at  $\chi = \pm\chi_{\max}(l)$  and form the double-valued behavior shown in Fig. 3(a). The first solution for  $f_-$  has a maximum and the second one a minimum at  $\chi = 0$  at a fixed  $l$ . The same occurs at  $l \rightarrow 0$  at a fixed  $\chi$ , where the minimum is zero.

If  $\chi$  were fixed experimentally, the first solution would describe the stable and the second one the metastable states. However, the control parameter in experiments is usually  $\phi$ . After switching over from  $\chi$  to  $\phi$ , the order parameter is described by the continuous single-valued dependence  $f_-(\phi, l)$  shown in Fig. 3(b). The first solution operates in the region  $|\phi| \in [0, \phi_*(l)]$  while the other one is in  $|\phi| \in [\phi_*(l), \pi]$ . Here,  $\phi_*(l) \approx \frac{\pi}{2} + \arcsin(\frac{1}{\cosh l})$ . The adjoining regions do not overlap due to a substantial phase incursion occurring at small  $f$ . The curves' crossing, seen in Fig. 3(b) at small  $f_-$ , is a manifestation of the opposite behavior of the two solutions with increasing  $l$ . If  $\phi = \pi$ ,  $f$  is zero at  $x = 0$  at arbitrary  $l$ , that allows phase-slip processes in the central lead [19,27,36].

For tunnel interfaces one obtains  $f_- \sim g_\ell f_+ \ll 1$  at  $g_{n,\delta} \lesssim g_\ell$ , except for the first solution at sufficiently small  $l$ .

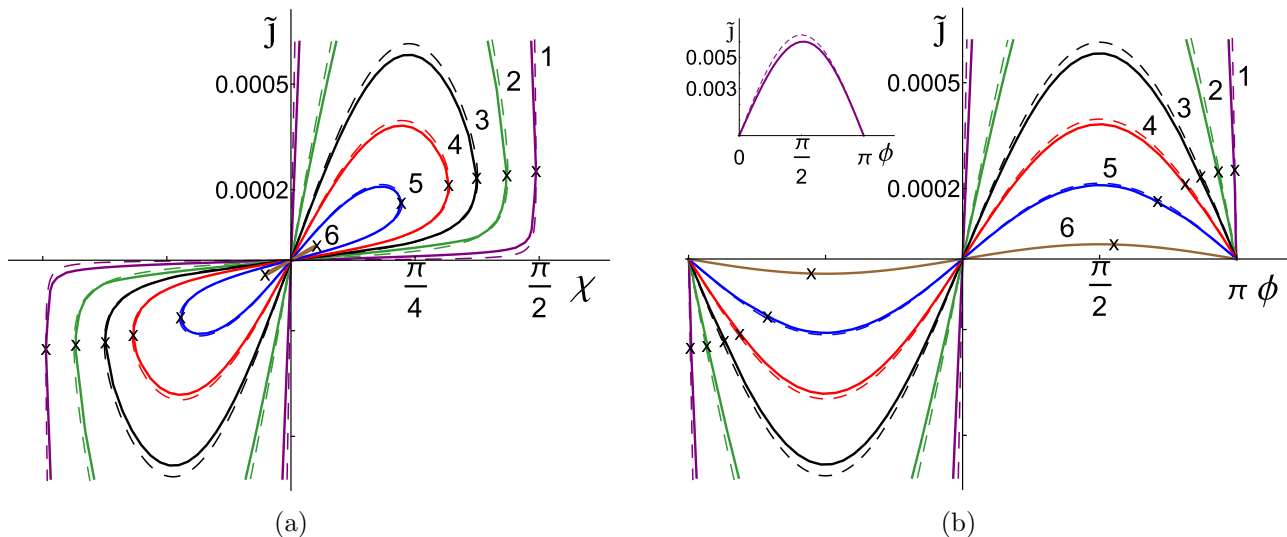


FIG. 4. Normalized supercurrent as (a) a double-valued function of  $\chi$  and (b) a single-valued function of  $\phi$  taken at various  $l$ : (1)  $l = 0.02$ , (2)  $l = 0.2$ , (3)  $l = 0.4$ , (4)  $l = 0.6$ , (5)  $l = 1$ , (6)  $l = 2.5$ . Inset: The supercurrent at  $l = 0.02$  (solid line) and its analytical description at small  $l$  (dashed line).

The latter results, in the limit  $l \rightarrow 0$ , in the relation  $f_- = \frac{g_\ell \cos \chi}{g_\ell + g_{n,\delta}} f_+$ , which also applies to SISIS junctions [37] and approximately describes the dependence on  $\chi$ . For the whole parameter set used in the figures  $f_+$  weakly changes with  $\chi$  and  $l$ :  $f_+^2 \in (0.972, 0.978)$ . If  $g_{n,\delta} \lesssim g_\ell$  and  $\cos \chi \sim 1$ , one obtains  $f_- \sim f_+$ , while in the opposite case  $g_{n,\delta} \gg g_\ell$  the relation is  $f_- \ll f_+$ . Since  $g_\ell$  for tunnel interfaces is proportional to the transmission coefficient  $g_\ell \propto \mathcal{D}$  [33–35], the above relation results in  $f_- \propto \mathcal{D}$ , if  $g_\ell \ll g_{n,\delta}$ , and in the  $\mathcal{D}$ -independent quantity  $f_-$  for  $g_\ell \gg g_{n,\delta}$ . The second solution vanishes in the limit  $l \rightarrow 0$ , and satisfies the relation  $f_- = g_\ell f_+ \tanh \frac{l}{2}$  at arbitrary  $l$  and  $\chi = 0$ . In the case of large  $l$  the two solutions coincide and the relation at  $\chi = 0$  is  $f_- = g_\ell f_+$  [36].

*The supercurrent.* The normalized supercurrent  $\tilde{j} = j/j_{dp}$  is depicted in Figs. 4(a) and 4(b) at various  $l$  as a function of  $\chi$  and  $\phi$ , respectively. With respect to  $\chi$ , the supercurrent is in the shape of a double loop that looks like a sloping figure eight composed of the two solutions. After switching over from  $\chi$  to  $\phi$  the current-phase relation acquires the conventional form. The dashed curves, that correspond to approximate analytical results [36], have the sinusoidal shape in Fig. 4(b). They deviate within several percent from the numerical results (solid curves).

A substantial role of the phase incursion in creating such a behavior can be understood as follows. The supercurrent  $\propto g_\ell f_- f_+ \sin \chi$  is influenced by the proximity effect together with  $f_-$ . If  $\phi$  were completely neglected, the value  $\phi = \pi$  would correspond to  $\chi = \frac{\pi}{2}$ . Since the proximity effect vanishes at  $\chi \rightarrow \frac{\pi}{2}$ , one gets  $f_- \rightarrow 0$  that could explain the zeroth supercurrent at  $\phi = \pi$ . However, as  $f_-$  is small in the vicinity of  $\phi = \pi$ , one gets a noticeable phase incursion that reduces the variation range  $|\chi| \leq \chi_{\max}(l) < \frac{\pi}{2}$  and excludes a possibility for  $\chi$  to reach  $\frac{\pi}{2}$  at any nonzero  $l$ . Instead, there appear two solutions of the GL equation providing a return

passage for  $\chi$ , from 0 to  $\chi_{\max}(l)$  and back, while  $\phi$  changes over  $(0, \pi)$ . As a result, the correspondence of  $\chi = 0$  to both  $\phi = 0$  and  $\phi = \pi$  is established. The phase relations in the SINIS systems do not result in the regime of interchanging modes with abrupt supercurrent changes, that can occur in SISIS junctions [37–39].

The small values of the order parameter and supercurrent, that are characteristic for the second solution and marked with crosses in Figs. 3 and 4, are specifically associated with the choice  $g_\ell = 0.01$  for the Josephson coupling constant, taken for demonstrating a quantitative agreement between the numerical and approximate analytical results. The effects discussed increase with  $g_\ell$  and remain qualitatively the same for  $g_\ell \lesssim 1$  [40]. Thus for  $g_\ell = 0.1$  instead of  $g_\ell = 0.01$ , the characteristic values of  $f_-^2$  and  $\tilde{j}$  increase in about 50–100 times.

The first solution is strongly modified at small distances  $l \lesssim 2g_\ell(b_n|a|/ba_n)^{1/2} \ll 1$ , for which the analytical description, based on the relation  $f_- = \frac{g_\ell \cos \chi}{g_\ell + g_{n,\delta}} f_+$  rather than on  $f_- \sim g_\ell f_+ \ll 1$ , has to be developed [36]. The inset in Fig. 4(b) shows the solid curve 1 as a whole ( $l = 0.02$ ). The analytical results deviate weakly from the solid curve. When  $g_{n,\delta} \ll g_\ell$ , one obtains  $j \propto \mathcal{D}$ . A remarkable feature is that the supercurrent dependence on the transparency gradually evolves into  $\mathcal{D}^2$  with increasing  $\phi$  up to about  $\phi_*$  at a fixed small  $l$ , due to the increase of the phase incursion with  $\phi$ . Similar supercurrent behavior also takes place for some other reasons, in particular, with the increasing distance  $l$  [8,29–31]. For the second solution one always obtains  $j \propto \mathcal{D}^2$ . Such a crossover is a fingerprint of the underlying physics associated with the phase-dependent proximity effect of the Josephson origin that generates the unconventional behavior of internal phase differences in SINIS junctions.

The research is carried out within the state task of ISSP RAS.

- [1] B. D. Josephson, Possible new effects in superconductive tunnelling, *Phys. Lett.* **1**, 251 (1962).
- [2] B. D. Josephson, Coupled superconductors, *Rev. Mod. Phys.* **36**, 216 (1964).
- [3] B. D. Josephson, Supercurrents through barriers, *Adv. Phys.* **14**, 419 (1965).
- [4] P. G. de Gennes, Boundary effects in superconductors, *Rev. Mod. Phys.* **36**, 225 (1964).
- [5] K. K. Likharev, Superconducting weak links, *Rev. Mod. Phys.* **51**, 101 (1979).
- [6] W. Belzig, F. K. Wilhelm, C. Bruder, G. Schön, and A. D. Zaikin, Quasiclassical Green's function approach to mesoscopic superconductivity, *Superlattices Microstruct.* **25**, 1251 (1999).
- [7] T. M. Klapwijk, Proximity effect from an Andreev perspective, *J. Supercond.* **17**, 593 (2004).
- [8] A. A. Golubov, M. Yu. Kupriyanov, and E. Il'ichev, The current-phase relation in Josephson junctions, *Rev. Mod. Phys.* **76**, 411 (2004).
- [9] V. T. Petrashov, V. N. Antonov, P. Delsing, and T. Claeson, Phase Controlled Conductance of Mesoscopic Structures with Superconducting "Mirrors", *Phys. Rev. Lett.* **74**, 5268 (1995).
- [10] S. Guéron, H. Pothier, N. O. Birge, D. Esteve, and M. H. Devoret, Superconducting Proximity Effect Probed on a Mesoscopic Length Scale, *Phys. Rev. Lett.* **77**, 3025 (1996).
- [11] P. Dubos, H. Courtois, B. Pannetier, F. K. Wilhelm, A. D. Zaikin, and G. Schön, Josephson critical current in a long mesoscopic S-N-S junction, *Phys. Rev. B* **63**, 064502 (2001).
- [12] W. Belzig, R. Shakhaidarov, V. V. Petrashov, and Yu. V. Nazarov, Negative magnetoresistance in Andreev interferometers, *Phys. Rev. B* **66**, 220505(R) (2002).
- [13] H. le Sueur, P. Joyez, H. Pothier, C. Urbina, and D. Esteve, Phase Controlled Superconducting Proximity Effect Probed by Tunneling Spectroscopy, *Phys. Rev. Lett.* **100**, 197002 (2008).
- [14] F. Giazotto, J. T. Peltonen, M. Meschke, and J. P. Pekola, Superconducting quantum interference proximity transistor, *Nat. Phys.* **6**, 254 (2010).
- [15] M. Meschke, J. T. Peltonen, J. P. Pekola, and F. Giazotto, Tunnel spectroscopy of a proximity Josephson junction, *Phys. Rev. B* **84**, 214514 (2011).
- [16] F. Giazotto and F. Taddei, Hybrid superconducting quantum magnetometer, *Phys. Rev. B* **84**, 214502 (2011).
- [17] A. Ronzani, C. Altimiras, and F. Giazotto, Highly sensitive superconducting quantum-interference proximity transistor, *Phys. Rev. Appl.* **2**, 024005 (2014).
- [18] S. D'Ambrosio, M. Meissner, C. Blanc, A. Ronzani, and F. Giazotto, Normal metal tunnel junction-based superconducting quantum interference proximity transistor, *Appl. Phys. Lett.* **107**, 113110 (2015).
- [19] A. Ronzani, S. D'Ambrosio, P. Virtanen, F. Giazotto, and C. Altimiras, Phase-driven collapse of the Cooper condensate in a nanosized superconductor, *Phys. Rev. B* **96**, 214517 (2017).
- [20] O. V. Skryabina, S. V. Egorov, A. S. Goncharova, A. A. Klimenko, S. N. Kozlov, V. V. Ryazanov, S. V. Bakurskiy, M. Yu. Kupriyanov, A. A. Golubov, K. S. Napolskii, and V. S. Stolyarov, Josephson coupling across a long single-crystalline Cu nanowire, *Appl. Phys. Lett.* **110**, 222605 (2017).
- [21] A. A. Abrikosov, On the magnetic properties of superconductors of the second group, *Zh. Eksp. Teor. Fiz.* **32**, 1442 (1957); On the magnetic properties of superconductors of the second group, *Sov. Phys. JETP* **5**, 1174 (1957).
- [22] P. G. de Gennes, Self-consistent calculation of the Josephson current, *Phys. Lett.* **5**, 22 (1963).
- [23] M. Tinkham, *Introduction to Superconductivity*, 2nd ed. (McGraw-Hill, New York, 1996).
- [24] G. Deutscher and P. G. de Gennes, in *Superconductivity*, edited by R. D. Parks (Dekker, New York, 1969), Vol. 2, p. 1005.
- [25] A. A. Abrikosov, *Fundamentals of the Theory of Metals* (North-Holland, Amsterdam, 1988).
- [26] A. F. Volkov, Weak coupling produced in superconductors by irradiation, *Zh. Eksp. Teor. Fiz.* **60**, 1500 (1971); Weak coupling produced in superconductors by irradiation, *Sov. Phys. JETP* **33**, 811 (1971).
- [27] H. J. Fink, Supercurrents through superconducting-normal-superconducting proximity layers. I. Analytic solution, *Phys. Rev. B* **14**, 1028 (1976).
- [28] The boundary conditions (7) in Ref. [26] do not apply to the systems with the interfacial contributions to the free energy, e.g., with the Josephson coupling. The boundary condition (5) in Ref. [27] is, in general, incorrect.
- [29] M. Yu. Kupriyanov and V. F. Lukichev, Influence of boundary transparency on the critical current of "dirty" SS'S structures, *Zh. Eksp. Teor. Fiz.* **94**, 139 (1988) [*Sov. Phys. JETP* **67**, 1163 (1988)].
- [30] M. Yu. Kupriyanov, A. Brinkman, A. A. Golubov, M. Siegel, and H. Rogalla, Double-barrier Josephson structures as the novel elements for superconducting large-scale integrated circuits, *Physica C* **326**, 16 (1999).
- [31] A. Brinkman and A. A. Golubov, Coherence effects in double-barrier Josephson junctions, *Phys. Rev. B* **61**, 11297 (2000).
- [32] Within the GL theory, the central and external leads should be considered, strictly speaking, as the superconductors with close critical temperatures, that satisfy the condition  $T_{c1} < T < T_{c2}$  (see, e.g., Ref. [25]). The applicability domain is expected to allow, in practice, lower  $T_{c1}$  and  $T$  as well, as this occurs in some other problems [41].
- [33] Y. S. Barash, Anharmonic Josephson current in junctions with an interface pair breaking, *Phys. Rev. B* **85**, 100503(R) (2012).
- [34] Y. S. Barash, Probing interfacial pair breaking in tunnel junctions based on the first and the second harmonics of the Josephson current, *Phys. Rev. B* **85**, 174529 (2012).
- [35] Y. S. Barash, Interfacial pair breaking and planar weak links with an anharmonic current-phase relation, *Pis'ma Zh. Eksp. Teor. Fiz.* **100**, 226 (2014); Yu. S. Barash, Interfacial pair breaking and planar weak links with an anharmonic current-phase relation, *JETP Lett.* **100**, 205 (2014).
- [36] See Supplemental Material at <http://link.aps.org/supplemental/10.1103/PhysRevB.99.140508> for details of the derivations, which includes Refs. [42, 43].
- [37] Y. S. Barash, Proximity-reduced range of internal phase differences in double Josephson junctions with closely spaced interfaces, *Phys. Rev. B* **97**, 224509 (2018).
- [38] R. De Luca and F. Romeo, Sawtooth current-phase relation of a superconducting trilayer system described using Ohta's formalism, *Phys. Rev. B* **79**, 094516 (2009).
- [39] J. Ali Ouassou and J. Linder, Spin-switch Josephson junctions with magnetically tunable  $\sin(\delta\varphi/n)$  current-phase relation, *Phys. Rev. B* **96**, 064516 (2017).
- [40] Since the microscopic estimation in the dirty limit is  $g_\ell \sim \bar{D}\xi(T)/l_{\text{imp}}$ , where  $\bar{D}$  is the transmission coefficient averaged

- over the Fermi surface and  $l_{\text{imp}}$  is the electron mean free path due to impurity scattering, the condition  $g_\ell \sim 1$  still corresponds to the case  $\bar{D} \ll 1$ .
- [41] I. Petković, A. Lollo, L. I. Glazman, and J. G. E. Harris, Deterministic phase slips in mesoscopic superconducting rings, [Nat. Commun.](#) **7**, 13551 (2016).
- [42] S. Wolfram, *The Mathematica Book*, 5th ed. (Wolfram Media, New York, 2003).
- [43] Y. S. Barash, Proximity-induced minimum radius of superconducting thin rings closed by the Josephson 0 or  $\pi$  junction, [Phys. Rev. B](#) **95**, 024503 (2017).